

In Every Issue

- 5 From the President**
by Steve Brachman
- 7 From the Editor**
by Bill Rizer
- 38 GeoEvents Calendar**
- 71 HGS Membership Application**
- 72 HGA/GeoWives**
- 73 Professional Directory**

Houston Geological Society

OFFICERS

Steve Brachman *President*
 Linda Sternbach *President-elect*
 Andrea Reynolds *Vice President*
 Cheryl Desforges *Treasurer*
 John Jordan *Treasurer-elect*
 Jennifer Burton *Secretary*
 Bill Rizer *Bulletin Editor*
 Steve Earle *Editor-elect*

DIRECTORS

Bob Merrill
 Bonnie Milne-Andrews
 Jim Doyle
 Erik Mason

HGS OFFICE STAFF

Sandra Babcock *Office Manager*
 Lilly Hargrave *Webmaster*
 Ken Nemeth *Office Committee Chairman*

EDITORIAL BOARD

Bill Rizer *Editor*
 Steve Earle *Editor-elect*
 Elsa Kapitan-White *Advisory Editor*
 James Ragsdale *Advisory Editor*
 Charles Revilla *Advisory Editor*
 Lilly Hargrave *Advertising Editor*
 Lisa Krueger *Design Editor*

The Houston Geological Society Bulletin (ISSN-018-6686) is published monthly except for July and August by the Houston Geological Society, 14811 St. Mary's Lane, Suite 250, Houston, Texas 77079-2916. Phone: 713-463-9476, fax: 281-679-5504

Editorial correspondence and material submitted for publication should be addressed to the Editor, Houston Geological Society Bulletin, 14811 St. Mary's Lane, Suite 250, Houston, Texas 77079-2916 or to Editor@hgs.org

Subscriptions: Subscription to this publication is included in the membership dues (\$24.00 annually). Subscription price for nonmembers within the contiguous U.S. is \$30.00 per year. For those outside the contiguous U.S. the subscription price is \$46.00 per year. Single-copy price is \$3.00. Periodicals postage paid in Houston, Texas.

POSTMASTER: Send address changes to Houston Geological Society Bulletin, 14811 St. Mary's Lane, Suite 250, Houston, Texas 77079-2916

Technical Meetings

- 17 HGS General Dinner Meeting**
The Revitalization of Sligo Field
- 19 HGS International Explorationists Dinner Meeting**
West Africa DHI's: Pushing the Envelope
- 21 HGS Environmental and Engineering Dinner Meeting**
- 23 SIPES Luncheon Meeting**
Exploration Trends in the TX, LA Gulf Coast—A 50,000 foot View
- 25 HGS North American Explorationists Dinner Meeting**
Lessons Learned from By-Passed Plays: Mississippian Mission Canyon Play, North Dakota; Shongaloo Field, Louisiana; Salawati Basin, Indonesia
- 27 Joint HGS and SPE Luncheon Meeting**
Frade Field Development, Deepwater Campos Basin, Brazil



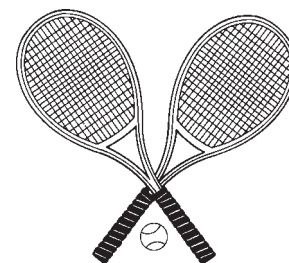
page 5



page 22

Other Features

- 5 New Office and Business Accounts Manager**
Welcome Sandra Babcock
- 7 In the News**
- 9 Letters to the Editor**
- 31 Scaled Experimental Models of Extension: Dry Sand vs. Wet Clay**
by Martha Oliver Withjack, Roy W. Schlische and Alissa A. Henza
- 50 Candidates for the 2007-2008 Executive Board**
- 61 Government Update**
by Henry M. Wise and Arlin Howles



page 24



page 28

BE SURE TO VOTE!

page 50

About the Cover: Normal faults in silic volcanic rock. Black Mountains, Death Valley, California. Reproduced with permission. Copyright Marii Bryant Miller, University of Oregon, visit www.marimillerphoto.com to see more of her excellent geological photographs. This photograph and many others can be viewed at the Earth Science World Image Bank, American Petroleum Institute, <http://www.earthscienceworld.org> an excellent source for geological photographs.

Scaled Experimental Models of Extension: Dry Sand vs. Wet Clay

by *Martha Oliver Withjack, Roy W. Schlische, and Alissa A. Henza*
Department of Geological Sciences, Rutgers University, Piscataway, NJ

Abstract

The choice of modeling material—dry sand or wet clay—affects the style and distribution of deformation in scaled experimental (analog) models of extension. For example, fault-zone widths are greater in sand than in clay, possibly reflecting the marked difference in maximum grain size of the modeling materials (<0.5 mm for dry sand vs. < 0.005 mm for wet clay). Most differences in the deformation patterns, however, reflect differences in the ductility of the modeling materials.

Normal faults are long, planar and hard-linked (i.e., directly connected) in the dry sand with its low ductility, whereas normal faults are short, curved and soft-linked (i.e., not directly connected) in the wet clay with its higher ductility. A few large normal faults accommodate most deformation in the sand models, whereas a few large faults and numerous small faults accommodate most deformation the clay models. Little folding occurs in the sand models, but folds are common in the clay models.

Introduction

For more than seventy-five years, geologists have used scaled experimental (analog) models to simulate extensional deformation in the upper crust (e.g., H. Cloos, 1928, 1930; E. Cloos, 1968; McClay and Ellis, 1987a, 1987b; Withjack et al., 1990, 1995; Withjack and Callaway, 2000; Schlische et al., 2002; Withjack and Schlische, 2006; Schreurs et al., 2006). These models provide valuable information about deformational processes. For example, they suggest how normal faults nucleate, propagate and link. Geologists can use this information to better understand a basin's petroleum system (e.g., its depositional patterns, migration pathways) and to minimize the uncertainties and risks associated with hydrocarbon exploration and production.

How well do these scaled experimental models simulate nature? The goal of this article is to address this fundamental question by looking at the influence of modeling materials on modeling results. First, we describe the key properties of the most common modeling materials—dry sand and wet clay—and discuss the basics of scaling. Second, we compare the results of sand and clay models for three common experimental setups of extensional deformation. Finally, we compare the results of the sand and clay models with natural examples of extensional deformation from rift basins and passive margins.

Modeling materials and scaling

The strength of most upper crustal rocks increases with depth, obeying a Mohr-Coulomb criterion of failure (e.g., Byerlee,

1978). According to this criterion,

$$\tau = C_0 + \mu\sigma_n \quad (1)$$

where τ and σ_n are, respectively, the shear and normal stresses on a potential fault surface, C_0 is the cohesive strength and μ is the coefficient of internal friction. This empirical criterion of failure describes the initiation of new faults, but not the reactivation of existing faults. For most sedimentary rocks, the coefficient of internal friction ranges from about 0.55 to 0.85 (e.g., Handin, 1966; Byerlee, 1978). For many intact sedimentary rocks, the cohesive strength is about 20 MPa (Handin, 1966), whereas for highly fractured sedimentary rocks, the cohesive strength is significantly less (e.g., Byerlee, 1978; Brace and Kohlstedt, 1980).

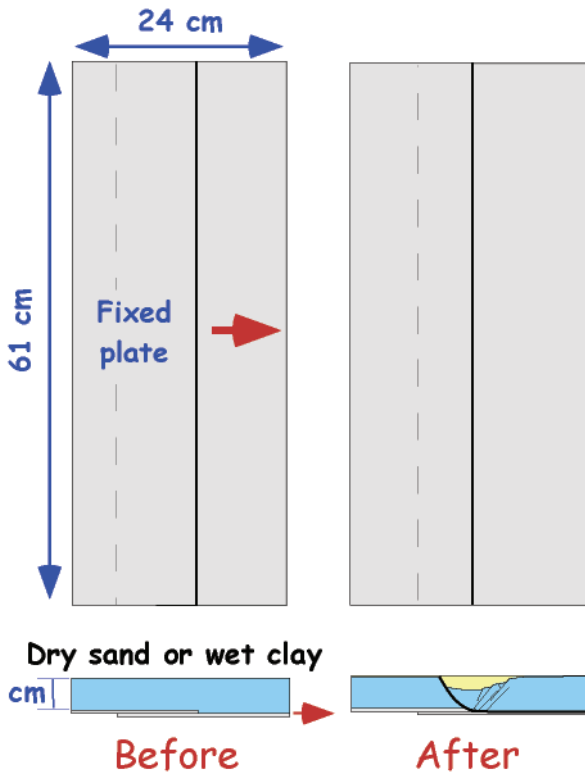
The two most common modeling materials used to represent upper crustal rocks are dry sand and wet clay. The dry sand is composed of fine quartz grains with diameters of less than 0.5 mm. The wet clay is composed predominantly of kaolinite particles (less than 0.005 mm in diameter) and water (~40% by weight). The properties of dry sand and wet clay are well documented (e.g., Richard and Krantz, 1991; Vendeville et al., 1995; Withjack and Callaway, 2000; Eisenstadt and Sims, 2005; Withjack and Schlische, 2006; Schreurs et al., 2006). Both modeling materials have similar densities ($\rho \sim 1600 \text{ kg m}^{-3}$). Like upper crustal rocks, both modeling materials have strengths that obey a Mohr-Coulomb criterion of failure. Their coefficients of internal friction are similar (0.5 for dry sand; 0.6 for wet clay), but their cohesive strengths are different (negligible for dry sand; ~50 Pa for wet clay).

Two conditions must be satisfied to create a scaled experimental model (e.g., Hubbert, 1937; Weijermars et al., 1993; Vendeville et al., 1995; Withjack and Callaway, 2000). First, the coefficient of friction of the modeling materials must be similar to that of upper crustal rocks. Second,

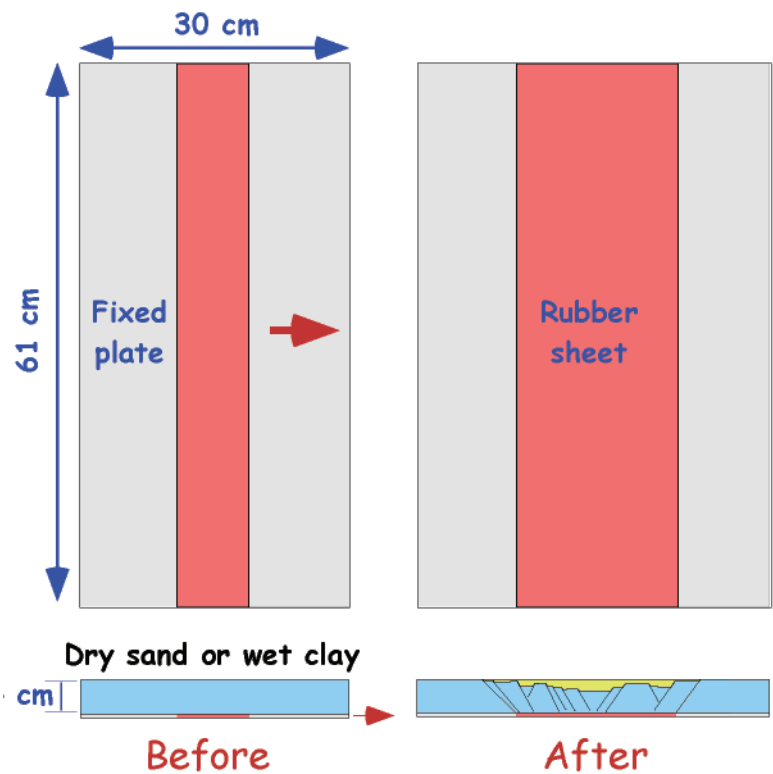
$$C_0^* = \rho^* \cdot g^* \cdot L^* \quad (2)$$

where C_0^* , ρ^* , g^* and L^* are ratios of model to natural prototype for cohesive strength, density, gravity, and length, respectively. In our models, the values of ρ^* and g^* are about 0.7 and 1, respectively, and L^* is 10^{-4} to 10^{-5} (i.e., 1 cm in the models equals 100 to 1000 m in nature). Thus, the second condition requires that the cohesive strength of the modeling materials must be approximately 10^{-4} to 10^{-5} of the cohesive strength of upper crustal rocks. These two conditions ensure that: 1) all forces, stresses and strengths in the models are scaled down by the same amount as the corresponding forces, stresses and strengths in nature, and 2) the strikes **Scaled Experimental Models of Extension** *continued on page 33*

Setup 1



Setup 2



Setup 3

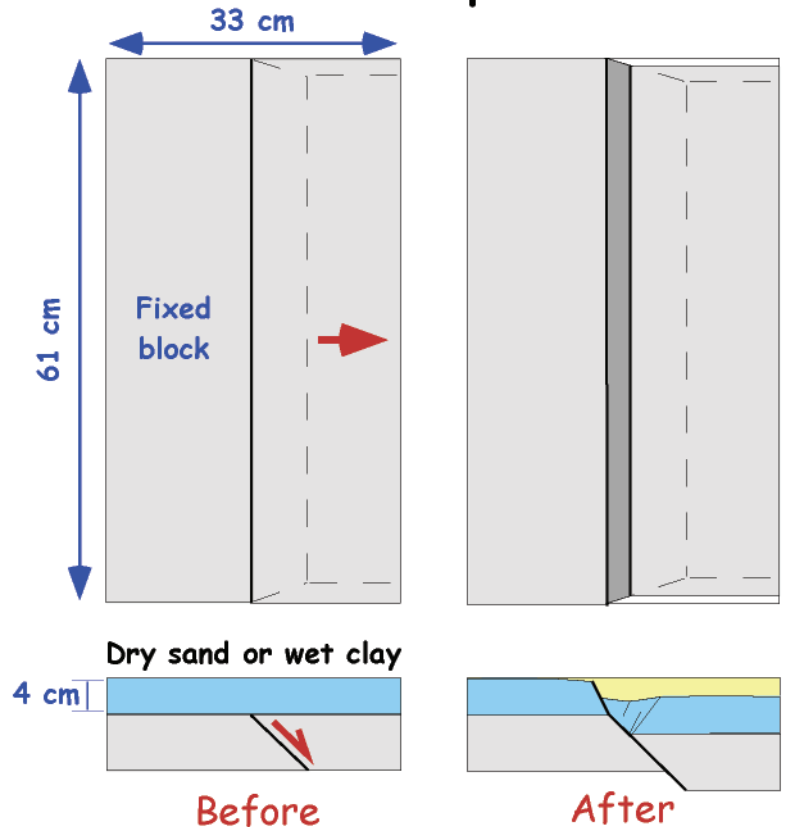


Figure 1. Experimental setups before and after deformation showing the map view (top) and a cross sectional view (bottom). In all models, a homogeneous layer of either dry sand or wet clay (blue), 4-cm thick, covers the flat base. Growth layers (yellow) fill in any depressions that form during the model runs. a) Setup 1: diverging, overlapping metal plates simulate a detached normal fault. Movement of the lower plate causes a normal fault to develop in the sand or clay layer. The fault emanates from the edge of the fixed upper plate. b) Setup 2: rubber sheet straddling diverging metal plates simulates distributed extension. Movement of one plate stretches the rubber sheet and the overlying sand or clay layer. In response, normal faults develop in the sand or clay layer. c) Setup 3: 45° dipping precut simulates a dipping normal fault. Movement along the precut creates a normal fault in the overlying sand or clay layer. The fault emanates from the edge of the fixed upper plate.

Scaled Experimental Models of Extension continued on page 35

and dips of the faults (relative to the principal stress axes) that develop in the models are similar to those in nature. Both conditions are satisfied with either dry sand or wet clay as the modeling material.

Although both dry sand and wet clay are suitable modeling materials to represent upper crustal rocks, they have different deformational styles related primarily to their different ductilities. Ductility reflects the capacity for distributed deformation at the scale of observation (Rutter, 1986). A great variety of deformation mechanisms ranging from fracturing/faulting to intracrystalline plasticity to diffusive mass transfer can produce ductile behavior (e.g., Rutter, 1986). In both dry sand and wet clay, the primary deformation mechanism is fracturing/faulting (e.g., Maltman, 1987; Richard and Krantz, 1991; Withjack and Callaway, 2000). Dry sand has a low ductility because most deformation is localized on a few major faults, even when strains are small. Wet clay has a high ductility because deformation is distributed on numerous minor to major faults. With increasing strain, however, most deformation becomes localized on a few major faults, even in the clay. To better understand the role of ductility on the results of scaled experimental models, we have compared the results from three identical models of extension using dry sand and wet clay as the modeling materials.

Experimental design

We have modeled extensional deformation using three common experimental setups (Figure 1). In all setups, a 4-cm thick, homogeneous layer of dry sand or wet clay overlies the flat base of the apparatus. In setup 1, two overlapping plates form the base of the apparatus. As the lower plate moves outward (at a constant rate), a normal fault propagates upward from the fixed edge of the upper plate through the overlying sand/clay layer. In setup 2, two plates form the base of the apparatus. An 8-cm wide sheet of rubber, attached to both plates, straddles the plate boundaries. As one plate moves outward (at a constant rate), the rubber sheet stretches and normal faults develop in the overlying sand/clay layer. In setup 3, two blocks separated by a 45° dipping precut surface form the base of the apparatus. As the hanging-wall block moves downward (at a constant rate), a normal fault propagates upward from the fixed edge of the footwall block through the overlying sand/clay layer. Photographs of the top surface of the models, taken at regular intervals, record the surface deformation through time. In several experiments, we fill in subsiding areas with either dry sand or wet clay at regular intervals to simulate deposition during deformation. These growth layers initially have a flat upper surface. After these experiments, we vertically slice the models, creating serial cross sections.

Comparison of sand and clay models

Similarities

Overall, fault patterns are similar in the sand and clay for all three experimental setups. High-angle (dipping 60°–65°) normal faults develop in both the dry sand and the wet clay (Figure 2). The faults strike approximately perpendicular to the extension direction in all models. For example, Figures 3a and 3b show the top surface of the sand and clay models for setup 2 (distributed extension) after 4 cm of displacement.

Differences

Deformation patterns differ in the sand and clay in several fundamental ways. Fault-zone widths are greater in the sand models than in the clay models (e.g., Figure 2a, right side). Faults in the sand are several millimeters wide, whereas faults in the clay are less than 0.1 mm wide. This difference in fault-zone width reflects the significant difference in the grain size of the modeling materials. Normal faults are long, relatively planar and hard-linked (i.e., directly connected to each other) in the sand models in both cross-sectional view (Figure 2) and map view (Figure 3). In the clay models, the normal faults are shorter, curved and soft-linked (i.e., not directly connected) in cross-sectional view (Figure 2) and map view (Figure 3). Previous work (Maltman, 1987) and recent studies (Granger et al., 2006) show that the surfaces of normal faults in the clay have numerous small-scale undulations that parallel the displacement direction (Figure 3e).

Fault distributions vary in the sand and clay models. Major faults accommodate most of the deformation in the sand models, whereas minor faults accommodate most deformation in the clay models. For example, 85% of the imposed displacement is accommodated by major faults, either the main normal fault or major secondary faults, in the sand model of setup 1 (Figure 2a). Only 15% of the imposed displacement is accommodated by minor secondary faults or cataclastic flow. In the corresponding clay model of setup 1, only 44% of the imposed displacement is accommodated by major faults, either the main normal fault or major secondary faults (Figure 2a). More than 55% of the imposed displacement is accommodated by minor secondary faults or by cataclastic flow.

Another major difference between the sand models and clay models is the lack of folds in the sand compared to the clay. Numerous relay ramps and fault-displacement folds develop in the clay where they provide displacement transfer between the normal faults that die out along strike. (e.g., Figure 3b, 3d, and 4a). Fault-bend folds also develop in the clay. For example, a faulted fault-bend fold (rollover fold) develops in the hanging wall of the main normal fault in the clay model of setup 1 (Figure 2a, bottom; Figures 4b, 4c). In contrast a series of relatively rigid fault blocks forms in the hanging wall of the main normal fault in the sand model of setup 1 (Figure 2a, top). As displacement on

Scaled Experimental Models of Extension continued from page 35

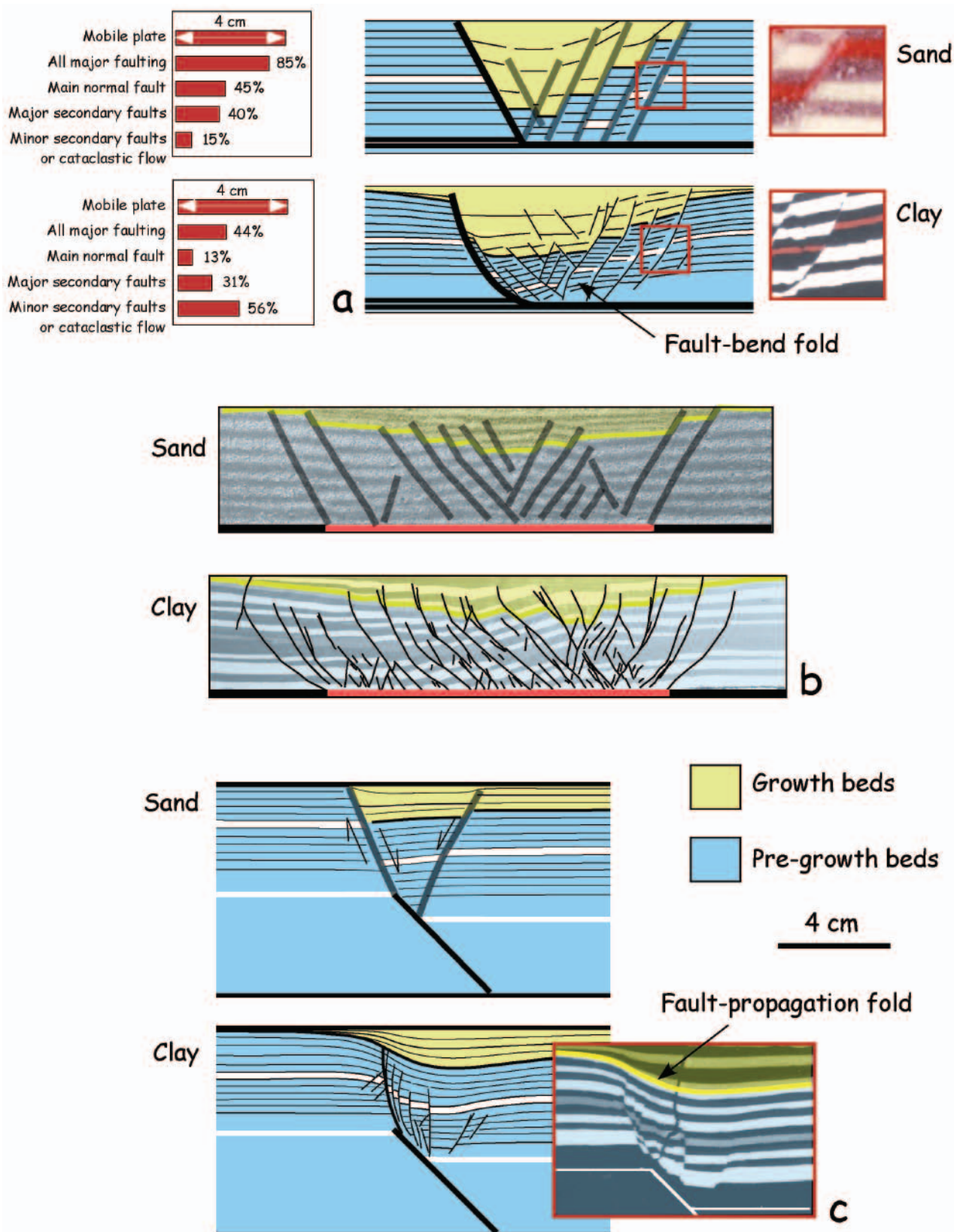


Figure 2. Cross sections through the sand and clay models for the three experimental setups. All cross sections are shown at the same scale. Black lines are interpreted faults. a) Cross sections through setup 1 for sand (top) and clay (bottom) after 4 cm of displacement on moving plate. The two photographs on the right show enlargements of fault zones from the models. The red outline boxes show the photographs' locations. Diagrams on the left show the distribution of deformation in the sand and clay models. b) Cross sections through setup 2 for sand (top) and clay (bottom) after 4 cm of stretching of the rubber sheet. c) Cross sections through setup 3 for sand (top) and clay (bottom) after 1.4 cm of displacement. The photograph on the right shows the faulting and folding in the clay model.

Scaled Experimental Models of Extension continued on page 41

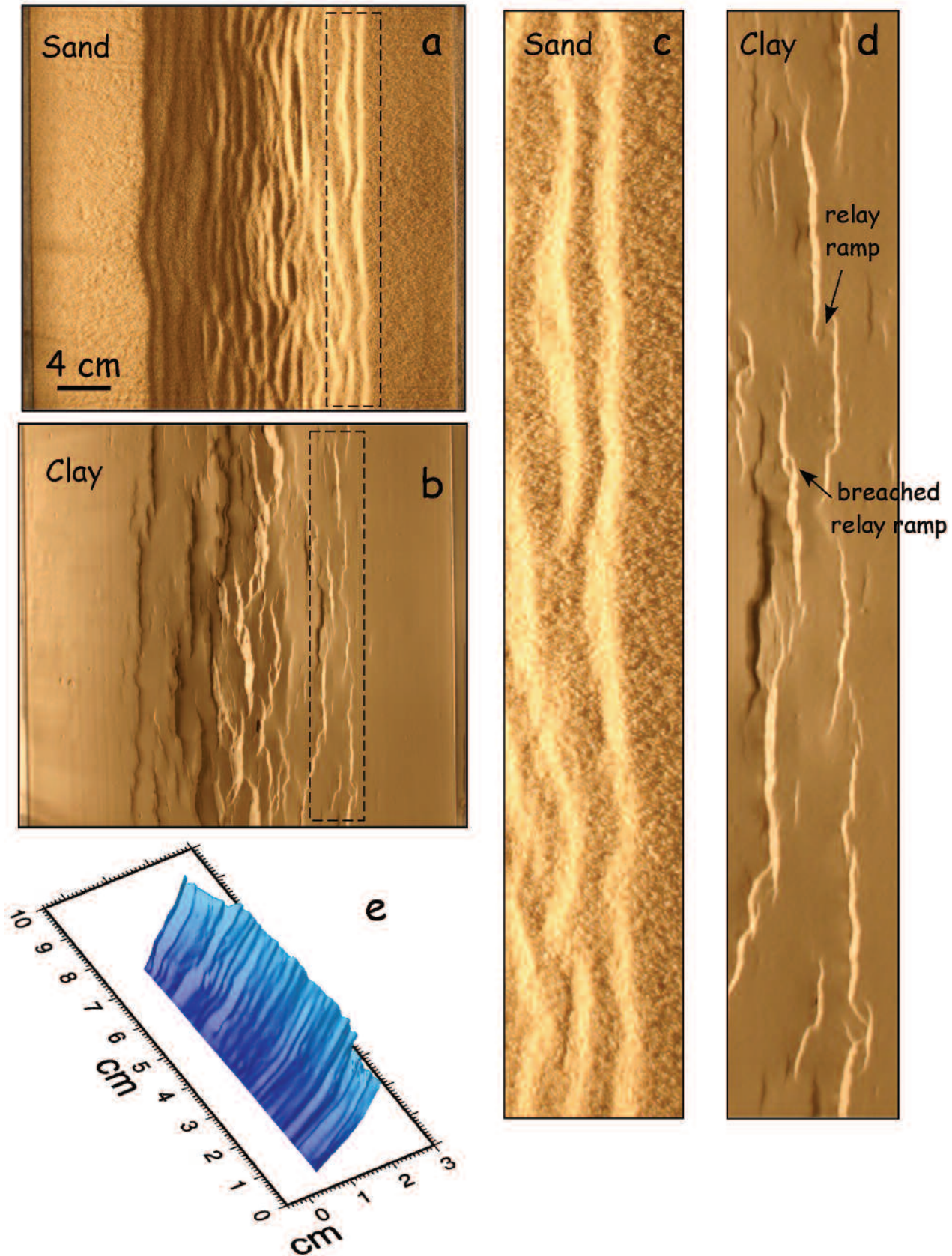


Figure 3. Map views of sand and clay models for setup 2 after 4 cm of stretching of the rubber sheet. a) Photograph of top surface of sand model. b) Photograph of top surface of clay model. c) and d) Close-up photographs of sand and clay models. The dashed lines in a) and b) show photographs' locations. e) Crenulations on a fault surface from clay model in setup 2 (after Granger et al., 2006).

Scaled Experimental Models of Extension continued on page 43

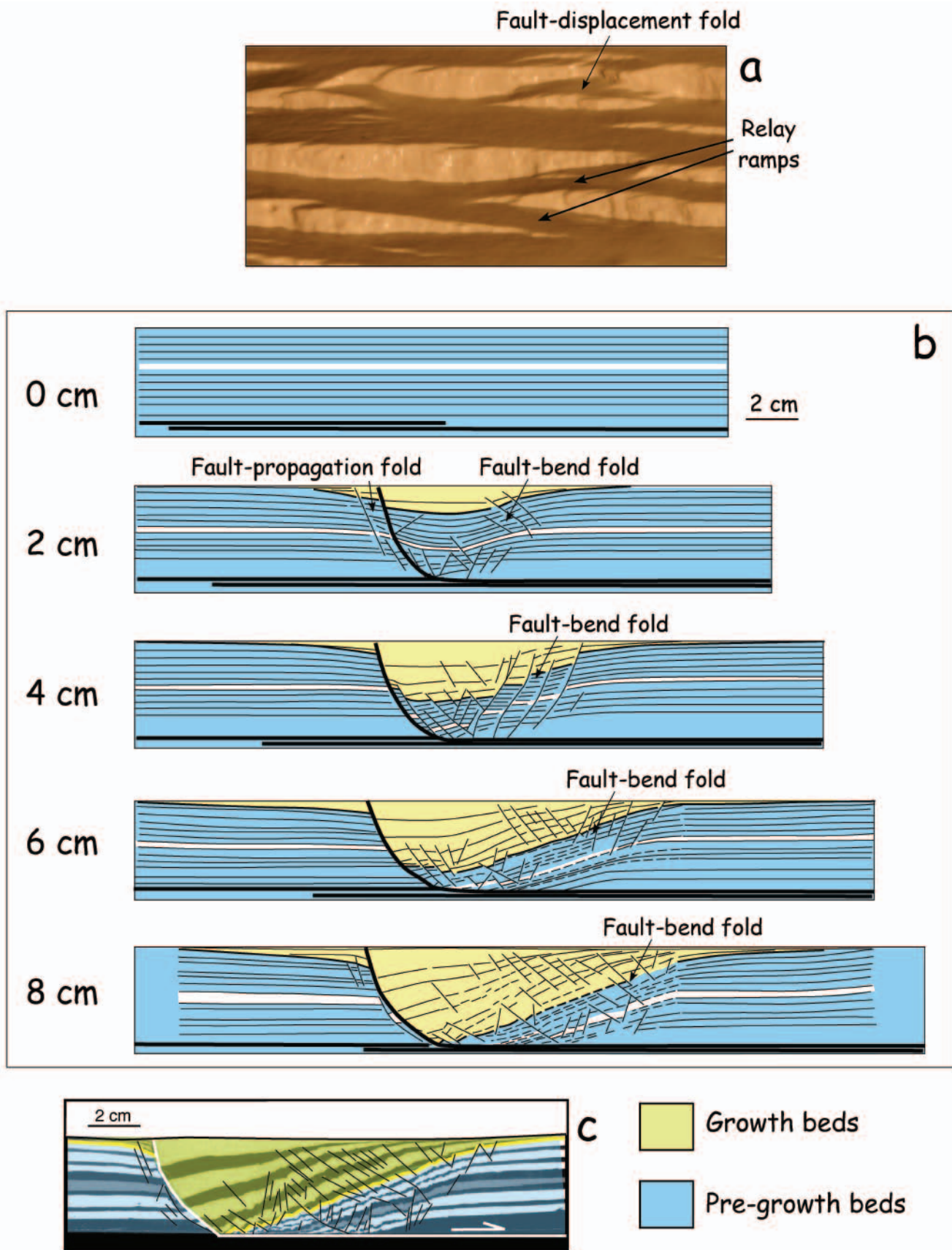


Figure 4. Cross sections of folds in the clay models. a) Relay ramps and fault displacement folds from setup 2. b) Development of fault-bend folds (rollover folds) from setup 1 as displacement of the moving plate increases from 0 to 8 cm. c) Photograph of clay model from setup 1 after 8 cm of displacement of the moving plate.

Scaled Experimental Models of Extension continued on page 45

the moving plate increases, the rollover fold in the clay grows wider, bedding dips increase and bedding thickness decreases (Figure 4b). Numerous minor to major normal faults accommodate the rollover folding. Fault-propagation folds also develop in the clay but not the sand. For setup 3, a major normal fault and a minor antithetic fault develop in the sand model (Figure 2c, top), whereas a fault-propagation fold develops in the identical clay model (Figure 2c, bottom). Numerous small-scale faults cut the folded beds (Figure 2c, photograph).

Summary and discussion

Overall, fault patterns are similar in the extensional sand and clay models in that high-angle normal faults develop that strike roughly perpendicular to the extension direction. Deformation patterns, however, have several fundamental differences. Individual fault-zone widths are much greater in the sand than in the clay, reflecting the significant difference in grain size of the modeling materials (< 0.5 mm for dry sand vs. < 0.005 mm for wet clay). Most differences in the deformation patterns, however, reflect the different ductilities of the modeling materials. Normal faults are long, planar and hard-linked in the sand, whereas they are shorter, curved and soft-linked in the clay. A few large normal faults accommodate most deformation in the sand models, whereas a few large faults and numerous minor faults accommodate most deformation in the clay models. Little folding occurs in the sand models, but folds (relay ramps, fault-displacement, fault-propagation and rollover) are numerous in the clay models.

Which modeling material best replicates nature? The answer to this question depends on the ductility of the natural example at the scale of observation. The dry sand, with its low ductility, best represents rock that deforms primarily by localized faulting. Figure 5a shows an outcrop from Greece where most deformation is localized on two fault zones. The localized deformation on the normal faults resembles that in the sand model of setup 3 (Figure 2c). The wet clay, with its greater ductility, best represents rock that deforms by distributed minor and major faulting. The distributed deformation on numerous normal faults of varying size and the presence of relay ramps and fault-displacement folds in the North Sea (Figure 5b) resembles the deformation patterns in the clay model of setup 2 (Figure 4a). The undulations on the fault surfaces are similar to those on the fault surfaces in the clay models (Figure 3e). The Blackberry normal fault in the Gulf of Mexico with its rollover fold cut by numerous small-scale normal faults (Figure 5c) resembles the deformation in the clay model of setup 1 (Figures 4b, 4c). The fault-propagation folds from the Gulf of Suez (Figures 5d, 5e) resemble the fault-propagation folds from the clay models of setup 3 (Figure 3c).

Do these conclusions have implications for cross-section restoration? Restorations of cross sections from sand and clay models suggest that the assumed angle of simple shear used in many

restoration programs depends on ductility (Withjack and Schlische, 2006). Specifically, the effective shear angle is similar to the dip of observed normal faults if the ductility is low. The effective shear angle, however, can differ significantly from the dip of the observed faults if the ductility is high. For example, in the sand model of setup 1, restorations show that the effective shear angle is 60°–65°, the same as the dip of the major antithetic faults (Figure 2a, top). In the clay model of setup 1, numerous minor to major normal faults (antithetic and synthetic) accommodate the hanging-wall deformation (Figure 2a, bottom). The effective shear angle (35°–50°) is considerably less than the dip of the antithetic normal faults, reflecting the combined effect of the antithetic and synthetic normal faults. ■

Acknowledgments

This research benefited from many thought-provoking discussions with Mark Baum, Jennifer Elder Brady, Amber Granger and William Rizer. NSF grant EAR-0408878 supported some of this research.

References

- Bally, A., Withjack, M., Meisling, K., and Fisher, D. 1991. Seismic expression of structural styles: Geological Society of America, Short Course Notes, 1991 National Meeting.
- Brace, W. F., and Kohlstedt, D. L., 1980, Limits on lithospheric stress imposed by laboratory experiments: *Journal of Geophysical Research*, v. 85, p. 6248–6252.
- Byerlee, J., 1978, Friction of rocks: *Pure Applied Geophysics*, v. 116, p. 615–626.
- Cloos, E., 1968, Experimental analysis of Gulf Coast fracture patterns: *AAPG Bulletin*, v. 52, p. 420–444.
- Cloos, H., 1928, Experimente zur inneren tektonik: *Centralblatt für Mineralogie, Abt. B*, p. 609–621.
- Cloos, H., 1930, Kunstliche gebirge, II: *Natur und Museum*, v. 60, p. 258–269.
- Eisenstadt, G., and Sims, D., 2005, Evaluating sand and clay models: do rheological differences matter? *Journal of Structural Geology*, v. 27, p. 1399–1412.
- Fault Analysis Group website, 2006, Available <http://www.fault-analysis-group.ucd.ie/>
- Gawthorpe, R. L., Sharp, I. R., and Underhill, J. R., 1997, Linked sequence stratigraphic and structural evolution of propagating normal faults:

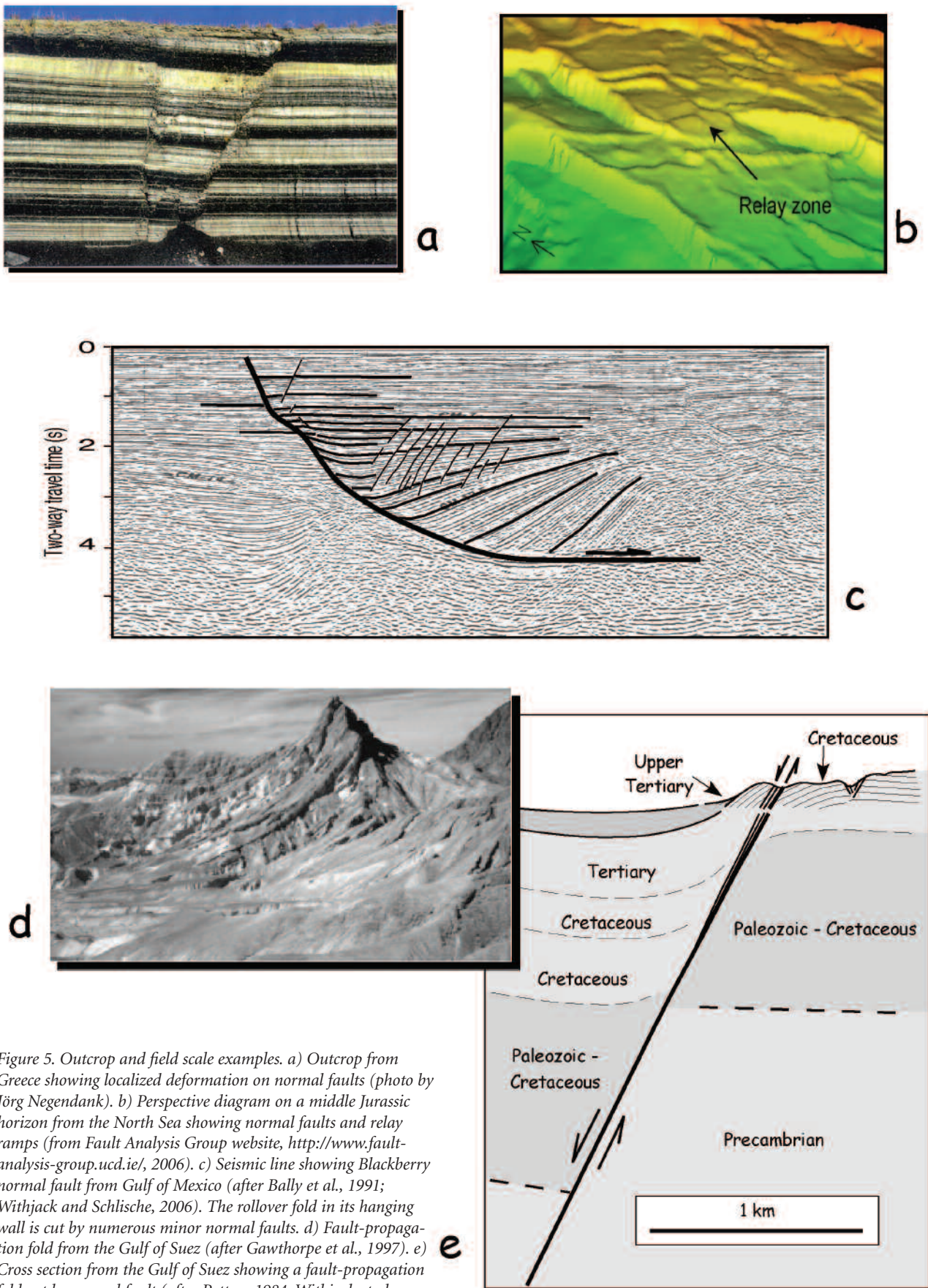


Figure 5. Outcrop and field scale examples. a) Outcrop from Greece showing localized deformation on normal faults (photo by Jörg Negendank). b) Perspective diagram on a middle Jurassic horizon from the North Sea showing normal faults and relay ramps (from Fault Analysis Group website, <http://www.fault-analysis-group.ucd.ie/>, 2006). c) Seismic line showing Blackberry normal fault from Gulf of Mexico (after Bally et al., 1991; Withjack and Schlische, 2006). The rollover fold in its hanging wall is cut by numerous minor normal faults. d) Fault-propagation fold from the Gulf of Suez (after Gawthorpe et al., 1997). e) Cross section from the Gulf of Suez showing a fault-propagation fold cut by normal fault (after Patton, 1984; Withjack et al., 1990). **Scaled Experimental Models of Extension** continued on page 49

Geology, v. 25, p. 795–798. The photograph in Figure 5 d) is from the cover of the issue of Geology referenced here.

Granger, A.B., Withjack, M.O., and Schlische, R.W., 2006, Undulations on normal-fault surfaces: insights into fault growth using scaled physical models of extension: Geological Society of America Annual Meeting, v. 38, p. 480.

Handin, J., 1966, Strength and Ductility, in S. P. Clark, Jr., ed., Handbook of Physical Constants: Geological Society of America Memoir 97, p. 223–289.

Hubbert, M.K., 1937, Theory of scale models as applied to the study of geologic structures: Geological Society of America Bulletin, v. 48, p. 1459–1519.

Maltman, A., 1987, Shear zones in argillaceous sediments—an experimental study, in M. E. Jones and R. M. F. Preston, eds., Deformation of Sediments and Sedimentary Rocks, Geological Society of London Special Publications No. 29, p. 77–87.

McClay, K. R. and Ellis, P. G., 1987a, Analogue models of extensional fault geometries, in M. P. Coward, J. F. Dewey and P. L. Hancock, eds., Continental Extensional Tectonics: Geological Society of London Special Publication No. 28, p. 109–125.

McClay, K. R. and Ellis, P. G., 1987b, Geometries of extensional fault systems developed in model experiments: Geology, v. 15, p. 341–344.

Patton, T. L., 1984, Normal-fault and fold development in sedimentary rocks above a pre-existing basement normal fault: Ph. D. Thesis, Texas A & M University, College Station, Texas, 164 p.

Richard, P., and Krantz, R. W., 1991, Experiments on fault reactivation in strike-slip mode: Tectonophysics, v. 188, p. 117–131.

Rutter, E. H., 1986, On the nomenclature of mode of failure transition in rocks: Tectonophysics, v. 122, p. 381–387.

Schlische, R. W., Withjack, M. O., and Eisenstadt, G., 2002, An experimental study of the secondary fault patterns produced by oblique-slip normal faulting: AAPG Bulletin, v. 86, p. 885–906.

Schreurs, G., Buitter, S. J. H., Boutelier, D., Corti, G., Costa, E., Cruden, A. R., Daniel, J.-M., Hoth, S., Koyi, H., Kukowski, N., Lohrmann, J., Ravaglia, A., Schlische, R. W., Withjack, M. O., Yamada, Y., Cavozzi, C., DelVentisetti, C., Elder Brady, J. A., Hoffmann-Rothe, A., Mengus, J.-M., Montanari, D., and Nilfouroshan, F., 2006, Analogue benchmarking—results of shortening and extension experiments: Geological Society of London Special Publication No. 253, p. 1–27.

Vendeville, B., Withjack, M., and Eisenstadt, G., 1995, Introduction to experimental modeling of tectonic processes: Geological Society of

America, Short Course Notes, 1995 National Meeting, 120 p.

Weijermars, R., Jackson, M. P. A., and Vendeville, B., 1993, Rheological and tectonic modeling of salt provinces: Tectonophysics, v. 217, p. 143–174.

Withjack, M. O., and Callaway, J. S., 2000, Active normal faulting beneath a salt layer: An experimental study of deformation in the cover sequence: AAPG Bulletin, v. 84, p. 627–652.

Withjack, M. O. and Schlische, R. W., 2006, Geometric and experimental models of extensional fault-bend folds: Geological Society of London Special Publication No. 253, p. 285–305.

Withjack, M. O., Olson, J., and Peterson, E., 1990, Experimental models of extensional forced folds: AAPG Bulletin, v. 74, p. 1038–1054.

Withjack, M. O., Islam, Q., and Appointee, P., 1995, Normal faults and their hanging-wall deformation—an experimental study: AAPG Bulletin, v. 79, p. 1–18.

ASSOCIATION FOR WOMEN GEOSCIENTISTS • HOUSTON, TX ANNOUNCEMENT OF SCHOLARSHIP

The Association for Women Geoscientists (AWG) Lone Star Rising Scholarship provides professional development funding for women in the geoscience profession who wish to resume their geoscience careers after having been out of the work force for at least 2 years.

The awards are intended to cover professional development costs, up to \$500, such as enrollment in geoscience training courses or workshops, fees for certifications & licensing, conference fee & expenses, professional membership fees, or any other justifiable costs to help candidates reenter the workforce. The application due date is June 1st, 2007 and AWG membership is not required. More information can be found on our website <http://awglonestartx.blogspot.com>.

AWG Mission



The Association for Women Geoscientists is an international organization devoted to enhancing the quality and level of participation of women in the geosciences and to introducing girls and young women to geoscience careers. Membership is open to all who support AWG's goals. The Lone Star Chapter was re-established in 2002. The chapter holds monthly networking dinners in and around Houston and supports the “Lone Star Rising Scholarship.” ■